REALIZATION OF POROUS SILICON MULTILAYER BANDPASS FILTERS IN MID-INFRARED RANGE

***S. H. Badri[1], Alireza Salehi[2]**

[1] Department of Electrical Engineering, Sarab Branch, Islamic Azad University, Sarab, Iran

[2] Laboratory of Device Fabrication, Department of Electrical Engineering, K.N. Toosi University of Technology, IRAN

*Corresponding Author: hadi.badri@gmail.com

ABSTRACT: *Porous silicon is transparent up to 100 µm which makes it an ideal material for IR filter applications. Porous silicon multilayer filters don't suffer from delamination and they could be operated in space and at cryogenic temperatures. Porous silicon multilayer bandpass filter is fabricated by electrochemical etching of p-type silicon. Layers with different porosities were formed by applying current densities of 5-50 mA.cm^{-2} in a solution of aqueous 38%wt HF and ethanol (2:3) electrolyte. Filters presented in this paper have transmission peak wavelengths at 11.44 and 14.62µm and the full width at half maximum (FWHM) are 0.19 and 0.21µm, respectively.*

Keywords: Porous silicon, Multilayer, Bandpass, Optical filter

INTRODUCTION

The number of materials that are transparent, stable, and consistent with each other in the range of IR are limited. Multilayer thin film filters that are fabricated with different materials suffer from delamination, weak adhesion between multilayer and substrate, and compressive or tensile stress in layers which causes cracks. However, porous silicon offers tunable refractive index, relatively simple and cost effective fabrication, compatibility with available silicon industry, and operability in cryogenic temperatures [1,2].

Bandpass multilayer filters are based on interference of incident radiation between the layers. This is a simple bandpass configuration which is used:

$$(LH)^{p}\,LL\,(HL)^{p-1}\,H \qquad (1)$$

where L denotes a layer with low refractive index and H denotes a layer with high refractive index, and p is the number of repeating periods. Optical thickness of L and H Layers in bandpass interference filter should be equal to one-fourth of peak wavelength:

$$n_L d_L = n_H d_H = \frac{\lambda_p}{4} \qquad (2)$$

where n_L is refractive index and d_L physical thickness of L layers, similarly n_H and d_H correspond to H layers, and λ_p is a peak wavelength [3].

POROUS SILICON MULTILAYER

Porous silicon has caught the attention of researchers in recent years. Porous silicon has been used as varieties of optical filters [4], biosensors [5], photonic crystals [6] and drug delivery component [7]. Porous silicon multilayers are produced by changing one of the etching parameters periodically. Etching parameters that affect the morphology and pores' depth are current density, electrolyte composition, sample's doping, etc.

In producing porous silicon multilayers it should be considered that anodization process is self-limited by depletion of holes from porous silicon skeleton which is caused by quantum confinement. Once a porous silicon layer is formed anodization stops in this layer and only proceeds in pore tips. The porosity of layers depends only on current density when other etching parameters are kept fixed. Changing the current density results in layers with different porosities in depth of sample [8]. Fabrication of porous silicon layers by alternating the current density is illustrated in figure 1. Thickness and porosity of the porous silicon layer is proportional to applied current density and its duration. Etching rate depends on substrate's doping, electrolyte composition, illumination during etching, temperature and current density. Dependence of etching rate on current density, while other parameters are kept constant, is approximately a linear function.

The effective refractive index of porous silicon layer, n, depends on its porosity. The refractive index is almost a linear function of porosity [9]. Bruggeman approximation is used to determine the effective refractive index of porous silicon layer:

$$(1-p)\frac{\varepsilon_{Si}-\varepsilon_{PSi}}{\varepsilon_{Si}+2\varepsilon_{PSi}} + P\frac{\varepsilon_{air}-\varepsilon_{PSi}}{\varepsilon_{air}+2\varepsilon_{PSi}} = 0 \qquad (3)$$

where p is the porosity, and ε_{air}, ε_{Si}, ε_{PSi} are the dielectric constants of air, silicon, and porous silicon, respectively.

EXPERIMENTAL

The samples presented in this paper are prepared by electrochemical anodic etching of boron-doped silicon (100) with resistivity of 0.01-0.02 Ω.cm in a solution of aqueous 38%wt HF and ethanol (2:3) electrolyte.

The electrochemical cell is made of Teflon and Si sample is placed on Cu plate which acts as anode and an O-ring is used to ensure that only the front side of the sample is exposed to electrolyte. Platinum is placed in electrolyte as cathode. Pt and Teflon are resistant to HF. Schematic of the electrochemical etching cell is shown in figure 2. Before anodization, the Si samples are ultrasonically cleaned according to standard cleaning process. Anodization is performed by alternating the current density, without illumination and in ultrasonic device. Current is set to zero for a minute before each current change, allowing HF concentration to reach equilibrium at etch front. To have a free-standing porous silicon multilayer a high current density pulse is applied which results in electropolishing of a thin layer of silicon. After anodization samples were rinsed in ethanol and dried in ambient conditions in order to avoid cracks induced by capillary stress.

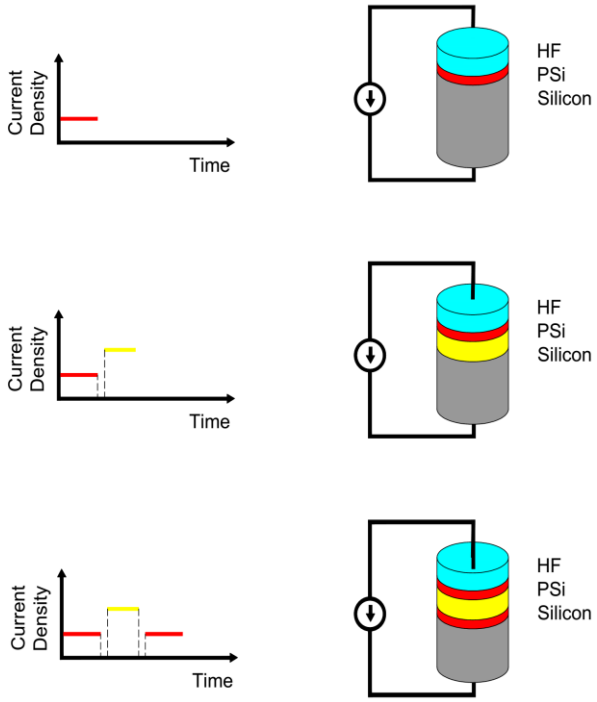

Fig. 1. Formation of porous silicon layers by applying different current densities. There is an interval between applying current densities to let the HF concentration at etch front to reach its equilibrium.

Employing data from [8] gave us an insight into typical etching rate, porosity, and related refractive index. Transmission spectra of samples were measured with FTIR instrument in laboratory of device fabrication of K.N. Toosi University of technology.

One simple way to recognize porous silicon multilayer is its appearance which tends to be bright and colored; on the contrary single layer porous silicon is dark.

Sample A

In sample A, $5mA/cm^2$ was applied for 155 seconds to produce layers with low porosity corresponding to high refractive index (denoted by H). Current density of $20mA/cm^2$ was applied for 42 seconds to produce layers with high porosity corresponding to low refractive index (denoted by L). At the end of the process $500mA/cm^2$ for 0.5 second was applied for electropolishing. The following configuration was used:

$$(LH)^{10}\ LL\ (HL)^{9}\ H \qquad (4)$$

Sample B

In sample B, $20mA/cm^2$ was applied for 55 seconds to produce layers with low porosity corresponding to high refractive index (denoted by H). Current density of $50mA/cm^2$ was applied for 25 seconds to produce layers with high porosity corresponding to low refractive index (denoted by L). At the end of the process $500mA/cm^2$ for 0.5 second was applied for electropolishing. The following configuration was used:

$$(LH)^{7}\ LL\ (HL)^{6}\ H \qquad (5)$$

Transmission spectra of samples are shown in figures 3 and 4.

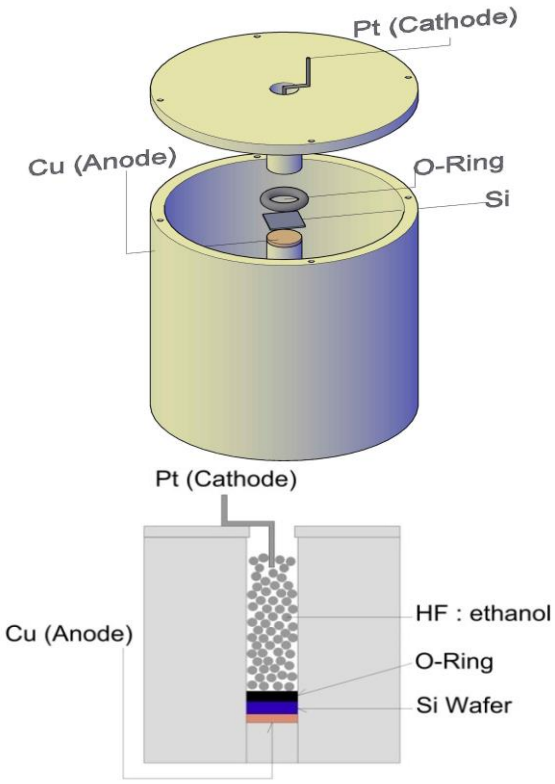

Fig. 2. Schematic of the electrochemical etching cell.

RESULTS AND DISCUSSIONS

Measured by gravitational method, porosity of layers in sample A are about 22% and 32% which correspond to refractive indices of 2.8 and 2.6, respectively. In sample B, porosity of layers are about 32% and 38% corresponding to refractive indices of 2.6 and 2.5, respectively.

Mismatches in optical thickness of layers results in lower transparency at λ_p, wider FWHM, and sidelobes in bandpass filters.

Optical thickness mismatch arises from the fact that HF concentration, at etch front, decreases slightly during anodization with a constant current. This decrease introduces higher porosity and lower etching rates as the depth of porous silicon layers or etching time increases. Although ultrasonic device was used to facilitate HF diffusion to etching front, the optical thickness mismatch of sample B is more pronounced because higher current is applied for its fabrication. This shows itself in higher transmission of sample B in sidelobes, compared to sample A.

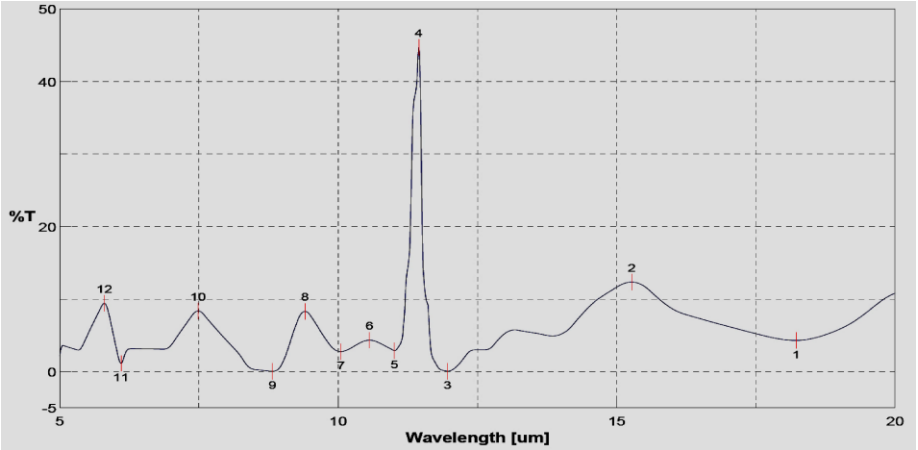

No.	um	%T	No.	um	%T	No.	um	%T
1	18.2266	4.30946	2	15.2738	12.3524	3	11.9619	0.0790124
4	11.4469	44.6815	5	11.0095	2.90577	6	10.561	4.34973
7	10.0494	2.75482	8	9.40248	8.31887	9	8.81882	0.057161
10	7.48264	8.39648	11	6.10055	1.15329	12	5.8003	9.42947

Fig. 3. Transmission spectrum of sample A, with peak transmission of 44.7% at 11.44 µm and FWHM of 0.19 µm.

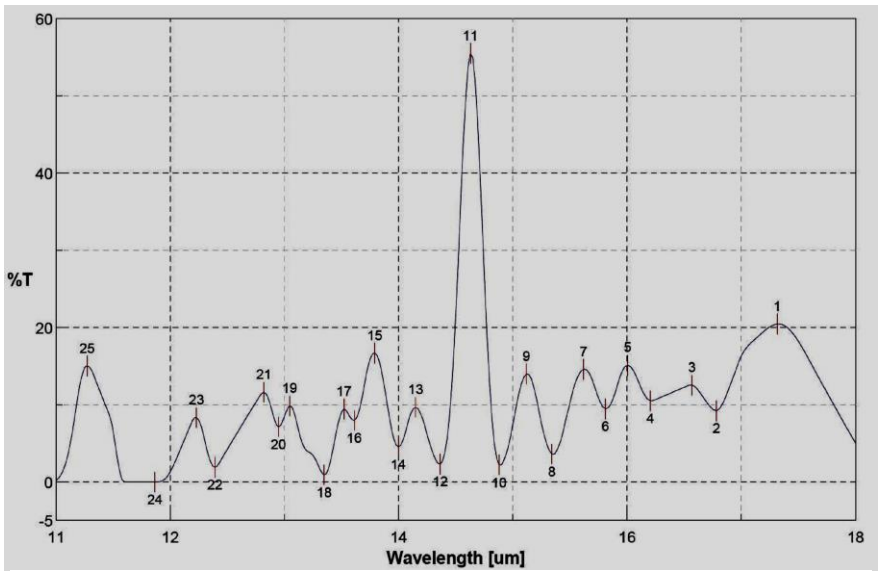

No.	um	%T	No.	um	%T	No.	um	%T
1	17.3137	20.4412	2	16.7814	9.22507	3	16.567	12.5376
4	16.2046	10.5225	5	16.0045	15.119	6	15.8093	9.45191
7	15.6189	14.6006	8	15.3416	3.60817	9	15.118	13.974
10	14.8794	2.21027	11	14.6275	55.5009	12	14.3642	2.32016
13	14.1486	9.65378	14	13.9959	4.5381	15	13.7911	16.6964
16	13.6101	7.99222	17	13.5214	9.42608	18	13.3474	0.913247
19	13.0452	9.84644	20	12.9475	7.1441	21	12.8194	11.6089
22	12.3906	1.90688	23	12.2299	8.3104	24	11.8661	4.34398E-005
25	11.2728	15.0076						

Fig. 4. Transmission spectrum of sample B, with peak transmission of 55.5% at 14.62 µm and FWHM of 0.21 µm.

As the number of layers increase, narrower FWHM could be achieved. However there is a trade-off between filter's transparency and FWHM, so number of layers can't be increased indefinitely. For higher ratio of n_H / n_L the FWHM of the sample decreases [8]. In sample A, this ratio and number of layers is higher than sample B so FWHM is narrower in sample A compared to sample B.

Temperature fluctuation during anodization is another source of change in porosity and etching rate, and consequently optical thickness mismatch in layers. It also contributes to interface roughness between layers which introduces perturbations in wavefront [10]. Temperature fluctuations are caused by resistive heating of sample and electrolyte due to the etching current and increase of water temperature in ultrasonic device. Sample B with higher etching current shows more pronounced sidelobes. Although water in ultrasonic device was changed continuously, temperature fluctuation is inevitable.

For improving the results, etching could be carried out in low temperature to decrease interface roughness and stirring process of electrolyte should be devised so that it wouldn't introduce any temperature change.

REFERENCES

[1] Christophersen, Marc, Vladimir Kochergin, and Philip R. Swinehart. "Porous silicon filters for mid-to far-IR range." *Optical Science and Technology, the SPIE 49th Annual Meeting. International Society for Optics and Photonics*, 2004.

[2] Kochergin, Vladimir, Mahavir Sanghavi, and Philip R. Swinehart. "Porous silicon filters for low-temperature far IR applications." *Optics & Photonics 2005. International Society for Optics and Photonics*, 2005.

[3] Macleod, Hugh Angus. Thin-film optical filters. *CRC Press*, 2001.

[4] Ma, Hui, and Hong-yan Zhang. "A compact dual-band bandpass filter based on porous silicon dual-microcavity of one-dimensional photonic crystal." *Optoelectronics Letters* 11: 95-99, 2015.

[5] Zhang, Hongyan, et al. "Porous silicon optical microcavity biosensor on silicon-on-insulator wafer for sensitive DNA detection." *Biosensors and Bioelectronics* 44: 89-94, 2013.

[6] Saplagio, Niel Gabriel E., et al. "Tunable Photonic Crystals Based on Electrochemically Etched Porous Silicon." *Int. J. Electrochem. Sci* 9: 6191-6200, 2014.

[7] Savage, David J., et al. "Porous silicon advances in drug delivery and immunotherapy." *Current opinion in pharmacology* 13.5: 834-841, 2013.

[8] Nalwa, H. S. Silicon-Based Material and Devices, *Academic Press*, 2001, Vol. 2, Ch. 4.

[9] Alvarado T, B., and V. Agarwal. "Optical Properties Of Random Dielectric Heterostructures Made Of Porous Silicon Multilayers." *Advances In Technology Of Materials And Materials Processing Journal* 9.2: 131, 2007.

[10] Setzu, S., P. Ferrand, and R. Romestain. "Optical properties of multilayered porous silicon." Materials Science and Engineering: B 69: 34-42 2000.